Simulations of Hydrogen Sorption in *rht*-MOF-1: Identifying the Binding Sites Through Explicit Polarization and Quantum Rotation Calculations

Tony Pham,[†,§] Katherine A. Forrest,[†,§] Adam Hogan,[†] Keith McLaughlin,[†]
Jonathan L. Belof,[‡] Juergen Eckert,[†] Brian Space[*,†]
[†]*Department of Chemistry, University of South Florida,*
4202 E. Fowler Ave., CHE205, Tampa, FL 33620-5250
[‡]*Lawrence Livermore National Laboratory,*
7000 East Ave., Livermore, CA 94550
[§]Authors contributed equally
[*]brian.b.space@gmail.com

Molecular Dynamics Simulations

Molecular dynamics (MD) simulations were performed to determine the equilibrium locations of the nitrate ions in *rht*-MOF-1. The as-synthesized crystal structure of *rht*-MOF-1 (taken from reference 1) revealed that the nitrate ions are located in the cuboctahedral cages (Figure 1(a)). It is deemed that the nitrate ions are positioned here because the solvent molecules are occupying more favorable sites in the as-synthesized structure. Thus, it is predicted that the removal of these solvent molecules will cause the nitrate ions to migrate to other regions of the MOF. In order to verify this, MD simulations were performed in the clean crystal structure of *rht*-MOF-1 (i.e., all solvent molecules were removed) using the nitrate ions as a moveable molecule. The simulations were performed at 77 K because this is the temperature of interest for the hydrogen sorption simulations in this work. The nitrate ion was parametrized using universal force field (UFF) parameters,[2] atomic point partial charges that were calculated using GAMESS[3] ($q_N = 1.0169\ e^-$, $q_O = -0.6723\ e^-$) and atomic point polarizabilities that were taken from van Duijnen *et al.*[4] The MD simulation was performed using an in-house modification of the Large-scale Atomic/Molecular Massively Parallel Simulator (LAMMPS) code[5,6] to include induced dipole interactions. The trajectories revealed that the nitrate ions migrate into the corners of the truncated tetrahedral cages (Figure 1(b)). These results are consistent to what was observed in a previous study.[7] The dynamics of the nitrate ions was characterized by the calculation of the mean-square displacement (MSD) from the simulation. The MSD is calculated by the following:

$$MSD = \frac{1}{N}\sum_{i=1}^{N} |\mathbf{r}_i(t) - \mathbf{r}_i(0)|^2 \qquad (1)$$

where N represents the total particle number, t is the time, and $\mathbf{r}_i(t)$ is the center-of-mass position of particle i at time t. The MSD plot for the nitrate ions in *rht*-MOF-1 is shown in Figure 2. A short MD trajectory video showing the displacement of the nitrate ions from their inital positions to their equilibrium positions in *rht*-MOF-1 can be found in the compressed folder for this manuscript. Note, the determination of the equilibrium positions of the nitrate ions in *rht*-MOF-1 at low temperatures was also verified through canonical Monte Carlo simulations.

Further, MD simulations were also performed with hydrogen molecules present in the MOF to see if the nitrate ions move from their equilibrium positions in the presence of adsorbate molecules at low temperatures. The simulations were performed at 77 K with 400 hydrogen molecules in the *rht*-MOF-1 unit cell with the nitrate ions located in the corners of the truncated tetrahedral cages. The trajectories revealed that the nitrate ions remain fixed in ther equilibrium locations even with the presence of the hydrogen molecules. The MSD plot demonstrating the movement of the nitrate ions in this MOF–H_2 system is shown in Figure 3. These results allowed us to perform the GCMC simulations of hydrogen sorption at 77 K and 87 K in *rht*-MOF-1 with the nitrate ions constrained to be rigid and localized in the corners of the truncated tetrahedral cages.

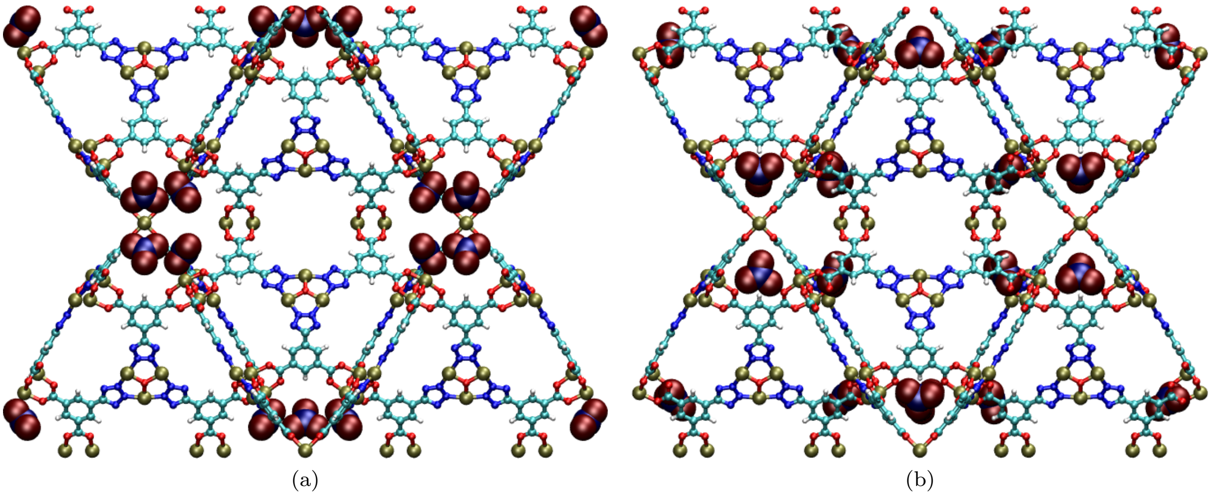

(a) (b)

Figure 1. The corner view of the *rht*-MOF-1 unit cell showing **(a)** the initial locations and **(b)** the equilibrium locations of the nitrate ions as determined from molecular dynamics simulations. MOF atom colors: C = cyan, H = white, N = blue, O = red, Cu = tan. Nitrate atom colors: N = dark blue, O = maroon.

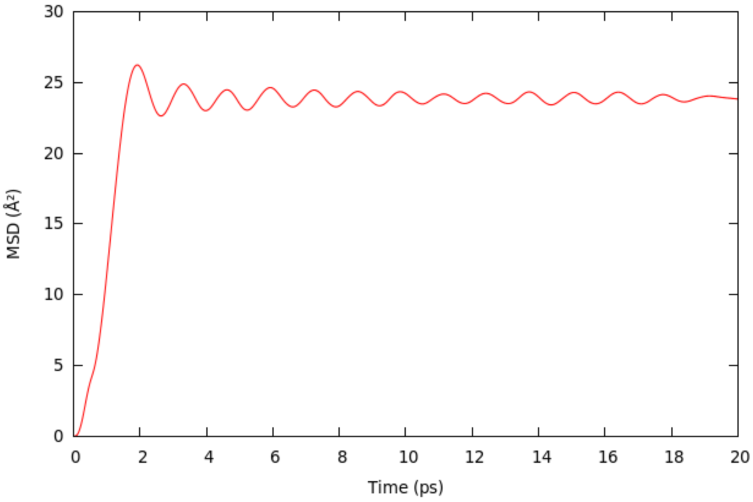

Figure 2. A plot of the mean-squared displacement (MSD) of the nitrate ions in *rht*-MOF-1 as a function of time calculated from molecular dynamics simulations. The temperature is 77 K.

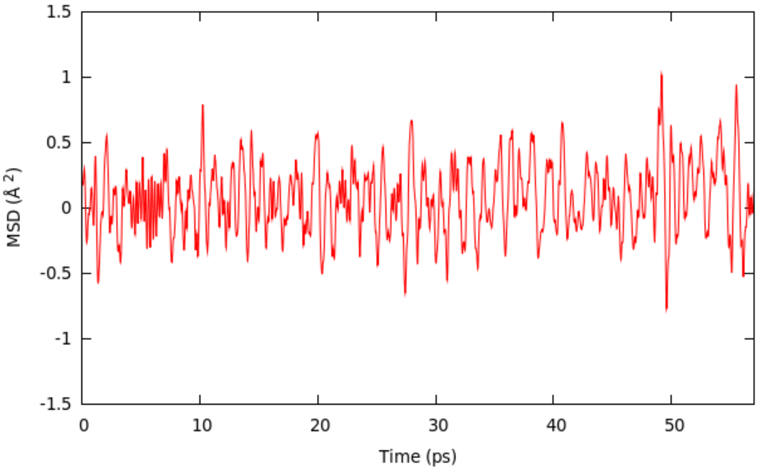

Figure 3. A plot of the mean-squared displacement (MSD) of the nitrate ions (positioned in the corners of the truncated tetrahedral cages) in *rht*-MOF-1 with the presence of hydrogen molecules of as a function of time calculated from molecular dynamics simulations. The temperature is 77 K.

Many-Body Polarization

In order to model hydrogen sorption in *rht*-MOF-1 accurately and effectively, the implementation of many-body polarization effects was required. This was included in the simulations by use of a Thole-Applequist type model.[8–10] An overview of the polarization model used in this work is given here.

Consider a static electric field applied to a system containing N atomic sites. The induced dipole, $\vec{\mu}$, at each site i is calculated *via* the following:

$$\vec{\mu}_i = \alpha_i^{\circ}\left(\vec{E}_i^{stat} + \vec{E}_i^{ind}\right) \tag{2}$$

where α° is the (scalar) atomic point polarizability, $\vec{E}^{stat}$ is the electrostatic field vector due to the atomic point partial charges of the MOF atoms and the adsorbate molecules, and $\vec{E}^{ind}$ is the electrostatic field vector due to the atomic induced dipoles. Equation 2 can be written in terms of the dipole field tensor, $\hat{\mathbf{T}}_{ij}$, as the following:

$$\vec{\mu}_i = \alpha_i^{\circ}\left(\vec{E}_i^{stat} - \sum_{j \neq i}^{N} \hat{\mathbf{T}}_{ij}\vec{\mu}_j\right) \tag{3}$$

In this work, the following dipole field tensor is used:

$$\hat{T}_{ij}^{\alpha\beta} \quad = \quad \nabla^{\alpha}\nabla^{\beta}\left(\frac{s(r)}{r_{ij}}\right) \tag{4}$$

where r_{ij} is the distance between sites i and j, and $s(r)$ is the screening function that serves to describe the charge distributions of the interacting dipoles, defined as:

$$s(r) = \left(\frac{\lambda r}{2} + 1\right)e^{-\lambda r} \tag{5}$$

where λ is a parameter damping the dipole interactions near the regions of discontinuity. A λ value of 2.1304 was used in this work, which is consistent with the work performed by Thole and others.[4,9,11]

Equation 3 can be solved by either matrix inversion or iterative methods. The latter was implemented in this work in order to increase computational speed. The Gauss-Seidel relaxation technique was the iterative method that was employed herein.[12] This method consists of updating the current dipole vector set for the ξ^{th} iteration step as the new dipole vectors become available:[11]

$$\vec{\mu}_i^{\xi} = \alpha_i^{\circ}(\vec{E}_i^{stat} - \sum_{j \neq i} \hat{T}_{ij}\vec{\mu}_j^{\xi-1+\zeta}) \tag{6}$$

$$\zeta = \begin{cases} 0, & \text{if } i < j \\ 1, & \text{if } i > j \end{cases} \tag{7}$$

The many-body polarization energy for the MOF–adsorbate system was calculated by the following based on the work of Palmo and Krimm[13] using the ξ^{th} iteration dipoles and the $(\xi + 1)^{th}$ induced field:

$$U_{pol}^{\xi} = -\frac{1}{2}\sum_i \vec{\mu}_i^{\xi} \cdot \vec{E}_i^{stat} - \frac{1}{2}\sum_i \vec{\mu}_i^{\xi} \cdot \vec{E}_i^{ind,\xi+1} \tag{8}$$

The dipoles were calculated and subjected to a spherical cut-off of 22.179 Å, which corresponds to half the unit cell dimension length. Note, in this work, MOF–MOF self-polarization was prohibited and only the induced field interactions between the MOF atoms and the hydrogen molecules were calculated.

Grand Canonical Monte Carlo

All simulations of hydrogen sorption in *rht*-MOF-1 were performed using grand canonical Monte Carlo (GCMC) on a single unit cell system of the MOF. This method constrains the chemical potential, volume, and temperature of the MOF–adsorbate system to be constant while allowing other thermodynamic quantities to fluctuate.[14] The simulation involves randomly inserting, deleting, translating, or rotating a adsorbate molecule with acceptance or rejection based on a random number generator scaled by the energetic favorability of the move. An infinitely extended crystal environment was approximated by periodic boundary conditions with a spherical cut-off of 22.179 Å, which corresponds to half the unit cell dimension length. All MOF atoms were constrained to be rigid during the simulations; this included the nitrate counterions, as it was shown through MD simulations that the nitrate ions are localized in the corners of the truncated tetrahedral cages at low temperatures (see previous section). In GCMC, the average particle number was calculated by the following expression:[15,16]

$$\langle N \rangle = \frac{1}{\Xi} \sum_{N=0}^{\infty} e^{\beta \mu N} \left\{ \prod_{i=1}^{3N} \int_{-\infty}^{\infty} dx_i \right\} N e^{-\beta U(x_1, \ldots x_{3N})} \tag{9}$$

where Ξ is the grand canonical partition function, β is the quantity $1/kT$ (k is the Boltzmann constant, T is the temperature), μ represents the chemical potential of the gas reservoir, and U is the total potential energy. The chemical potential for hydrogen was determined using the BACK equation of state.[17] The total potential energy of the MOF–adsorbate system was calculated by:

$$U = U_{rd} + U_{es} + U_{pol} \tag{10}$$

where U_{rd} is the repulsion/dispersion energy through use of the Lennard-Jones potential,[18] U_{es} is the electrostatic energy calculated by Ewald summation,[19] and U_{pol} is the many-body polarization energy as calculated by the Thole-Applequist model (equation 8).[8–10] For the simulations of hydrogen sorption at the temperatures considered in this work, quantum mechanical disperion effects were included semiclassically through the fourth order Feynman-Hibbs correction according to the following equation:[20]

$$U_{FH} = \frac{\beta \hbar^2}{24\mu} \left(U'' + \frac{2}{r} U' \right) + \frac{\beta^2 \hbar^4}{1152 \mu^2} \left(\frac{15}{r^3} U' + \frac{4}{r} U''' + U'''' \right) \tag{11}$$

where $\hbar$ is the reduced Planck's constant and the primes indicate differentiation with respect to pair separation r.

The absolute weight percent of hydrogen sorbed in the MOF was calculated by:

$$wt\% = \frac{\langle N \rangle m}{M + \langle N \rangle m} \tag{12}$$

where m is the molar mass of the adsorbate and M is the molar mass of the MOF.

The isosteric heats of adsorption, Q_{st}, were calculated based on the fluctuations in the particle number and the total potential energy in the system through the following expression:[21]

$$Q_{st} = -\frac{\langle NU \rangle - \langle N \rangle \langle U \rangle}{\langle N^2 \rangle - \langle N \rangle^2} + kT \tag{13}$$

For all state points considered, the simulations consisted of 1×10^6 Monte Carlo steps to guarantee equilibration, followed by an additional 1×10^6 steps to sample the desired thermodynamic properties and to ensure reasonable averages for the number of sorbed molecules and the Q_{st} values. All simulations were performed using the Massively Parallel Monte Carlo (MPMC) code,[22] which is currently available for download on Google Code.

Electronic Structure Calculations

Examination of the unit cell for *rht*-MOF-1 revealed 18 atoms (including those from the nitrate ion) in chemically distinct atomic environments (Figure 4). The atomic point partial charges for each chemically distinct atom were determined from electronic structure calculations on representational gas phase fragments that were large enough to mimic the chemical environment of the MOF. The chemical termination of each fragment was achieved by the addition of hydrogen atoms where appropriate. A total of three gas phase fragments were considered for *rht*-MOF-1 (Figure 5). Note, the nitrate ions were not included in the electronic structure calculations on the fragments because these counterions exhibit mobility in the MOF. Rather, the nitrate ion was treated as a separate system, as calculations were performed on a single nitrate ion in the gas phase to determine the partial charges of the atoms within the ion.

The GAMESS *ab initio* simulation package[3] was used to perform the quantum mechanical calculations on each fragment. Restricted open-shell Hartree-Fock methods were used for the open-shell fragments (Figures 5(a) and 5(b)), while restricted Hartree-Fock methods were used for the closed-shell fragment (Figure 5(c)). All light atoms were treated with the 6-31G* basis set to produce over-polarized charges appropriate for condensed phase simulation.[23] For the Cu^{2+} ions, the LANL2DZ[24–26] effective core potential basis set was used to treat the inner electrons of the many-electron species. The Connolly charge-fitting scheme[27] was used to perform the least-squared fit on the gas phase fragments. The partial charges for the chemically distinct atoms were in good agreement among the fragments. Thus, for each chemically distinct atom, the partial charges were averaged between the fragments and were assigned the point charge of the corresponding nuclear center of the atom. Note, for each fragment, the atoms that are located on the edges were not included in the averaging. The final calculated partial charges for each chemically distinct atom for *rht*-MOF-1 can be found in Table 1.

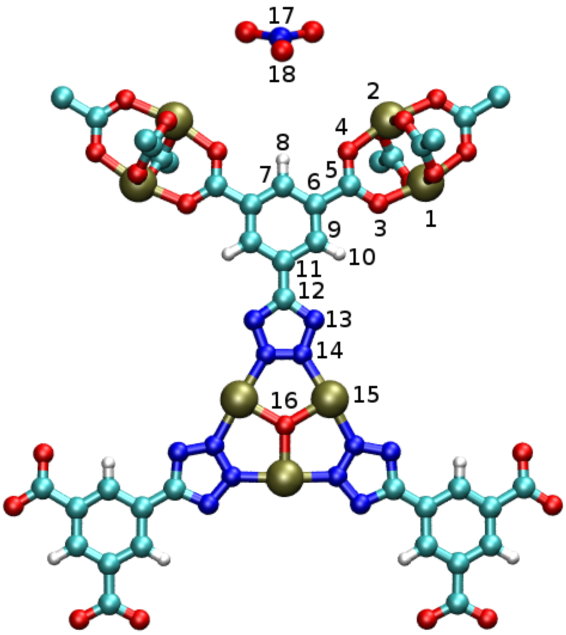

Figure 4. The numbering of the chemically distinct atoms in *rht*-MOF-1 as referred to in Table 1. Atom colors: C = cyan, H = white, N = blue, O = red, Cu = tan.

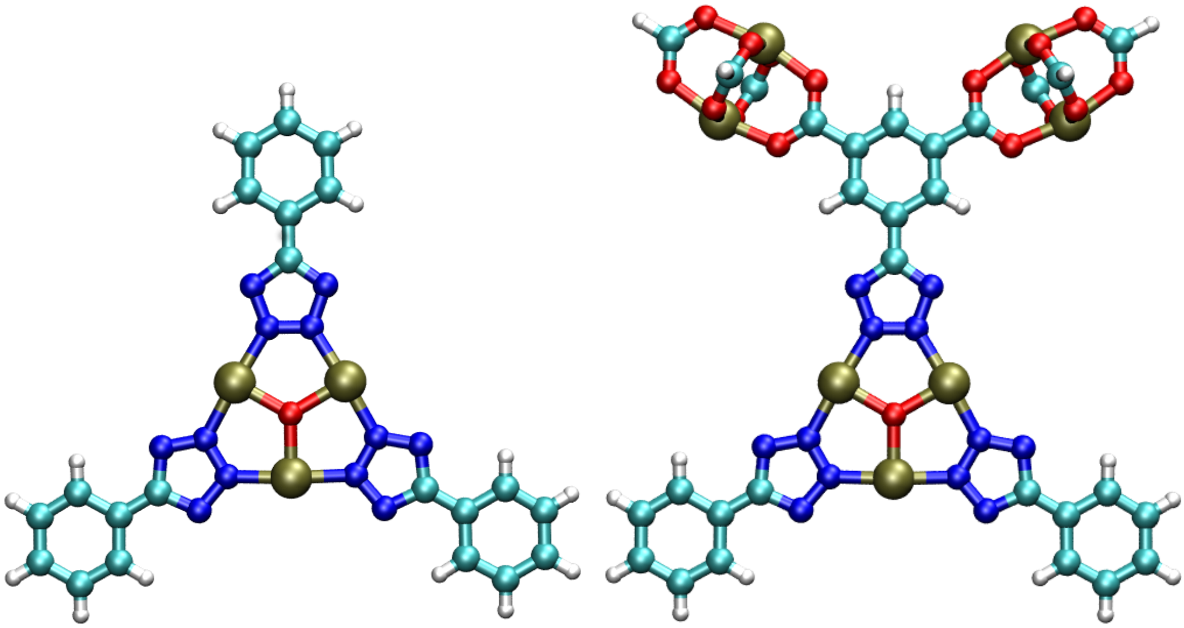

(a)Fragment 1

(b)Fragment 2

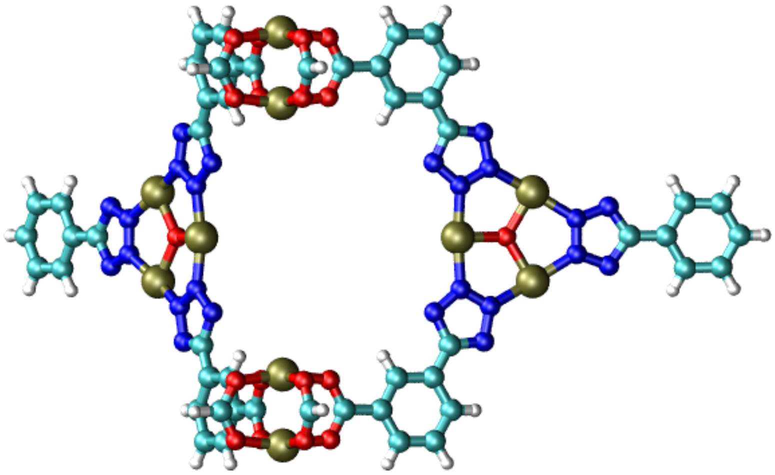

(c)Fragment 3

Figure 5. Representational gas phase fragments of *rht*-MOF-1 that were selected for charge fitting calculations. Atom colors: C = cyan, H = white, N = blue, O = red, Cu = tan.

Electronic Supplementary Material (ESI) for Journal of Materials Chemistry A
This journal is © The Royal Society of Chemistry 2014

Atom	Label	ϵ (K)	σ (Å)	q (e^-)	α° (Å^3)
Cu	1	2.51600	3.11400	1.55650	2.19630
Cu	2	2.51600	3.11400	1.06610	2.19630
O	3	30.19000	3.11800	-0.72860	0.85200
O	4	30.19000	3.11800	-0.73990	0.85200
C	5	52.84000	3.43100	0.96570	1.28860
C	6	52.84000	3.43100	-0.23590	1.28860
C	7	52.84000	3.43100	-0.00400	1.28860
H	8	22.14000	2.57100	0.15960	0.41380
C	9	52.84000	3.43100	0.26910	1.28860
H	10	22.14000	2.57100	0.03170	0.41380
C	11	52.84000	3.43100	-0.78730	1.28860
C	12	52.84000	3.43100	1.23930	1.28860
N	13	34.72000	3.26100	-0.50390	0.97157
N	14	34.72000	3.26100	-0.19120	0.97157
Cu	15	2.51600	3.11400	0.88400	2.19630
O	16	30.19000	3.11800	-0.61070	0.85200
N	17	34.72000	3.26100	1.01690	0.97157
O	18	30.19000	3.11800	-0.67230	0.85200

Table 1. The simulation parameters for *rht*-MOF-1. Label of atoms corresponds to Figure 4.

Hydrogen Potentials

Model	Atomic Site	r (Å)	ϵ (K)	σ (Å)	q (e^-)	α° (Å^3)
BSSP	H2G	0.00000	12.76532	3.15528	-0.74640	0.69380
	H2E	0.37100	0.00000	0.00000	0.37320	0.00044
	H2E	-0.37100	0.00000	0.00000	0.37320	0.00044
	H2N	0.36300	2.16726	2.37031	0.00000	0.00000
	H2N	-0.36300	2.16726	2.37031	0.00000	0.00000

Table 2. Parameters used to characterize the polarizable Belof Stern Space Polar (BSSP) hydrogen potential[28] used in this work. H2G corresponds to the center-of-mass site, H2E corresponds to the atomic locations of the hydrogen atoms, and H2N corresponds to the Lennard-Jones off-site.

Model	Atomic Site	r (Å)	ϵ (K)	σ (Å)	q (e^-)
Buch	H2G	0.00000	34.20000	2.96000	0.00000
DL	H2G	0.00000	36.70000	2.95800	-0.93600
	H2E	0.37000	0.00000	0.00000	0.46800
	H2E	-0.37000	0.00000	0.00000	0.46800
BSS	H2G	0.00000	8.85160	3.22930	-0.74640
	H2E	0.37100	0.00000	0.00000	0.37320
	H2E	-0.37100	0.00000	0.00000	0.37320
	H2N	0.32900	4.06590	2.34060	0.00000
	H2N	-0.32900	4.06590	2.34060	0.00000

Table 3. Parameters used to characterize three nonpolarizable hydrogen potentials for control simulations performed in this work: Buch model,[29] Darkrim-Levesque (DL) model,[30] and Belof Stern Space (BSS) model.[28] H2G corresponds to the center-of-mass site, H2E corresponds to the atomic locations of the hydrogen atoms, and H2N corresponds to the Lennard-Jones off-site.

Additional Data

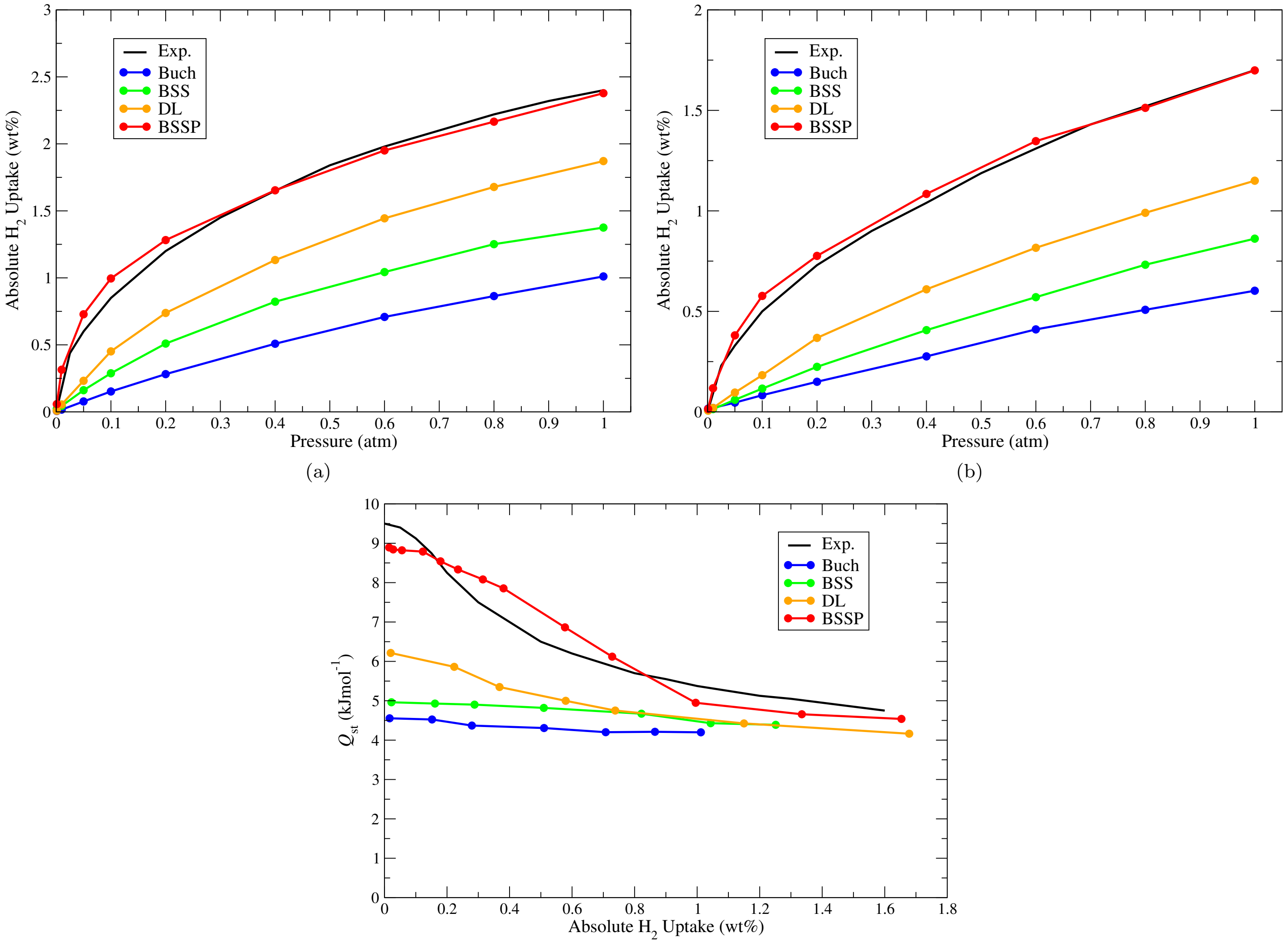

(a) (b)

(c)

Figure 6. Low-pressure (up to 1.0 atm) absolute hydrogen sorption isotherms in *rht*-MOF-1 at **(a)** 77 K and **(b)** 87 K for experiment (black), Buch model (blue), BSS model (green), DL model (orange), and BSSP model (red). **(c)** Isosteric heats of adsorption, Q_{st}, for hydrogen in *rht*-MOF-1 plotted against hydrogen uptakes.

[1] Nouar, F.; Eubank, J. F.; Bousquet, T.; Wojtas, L.; Zaworotko, M. J.; Eddaoudi, M. *Journal of the American Chemical Society* **2008**, *130*, 1833–1835.
[2] Rappé, A. K.; Casewit, C. J.; Colwell, K. S.; Goddard, W. A.; Skiff, W. M. *Journal of the American Chemical Society* **1992**, *114*, 10024–10035.
[3] Schmidt, M. W.; Baldridge, K. K.; Boatz, J. A.; Elbert, S. T.; Gordon, M. S.; Jensen, J. H.; Koseki, S.; Matsunaga, N.; Nguyen, K. A.; Su, S.; Windus, T. L.; Dupuis, M.; Montgomery, J. A. *Journal of Computational Chemistry* **1993**, *14*, 1347–1363.
[4] van Duijnen, P. T.; Swart, M. *The Journal of Physical Chemistry A* **1998**, *102*, 2399–2407.
[5] Plimpton, S. *Journal of Computational Physics* **1995**, *117*, 1–19.
[6] Hogan, A.; Space, B. LAMMPS Induced-Dipole Polarization Pair Style. Available on Google Code, 2013.
[7] Babarao, R.; Eddaoudi, M.; Jiang, J. W. *Langmuir* **2010**, *26*, 11196–11203.
[8] Applequist, J.; Carl, J. R.; Fung, K.-K. *Journal of the American Chemical Society* **1972**, *94*, 2952–2960.
[9] Thole, B. *Chemical Physics* **1981**, *59*, 341 – 350.
[10] Bode, K. A.; Applequist, J. *The Journal of Physical Chemistry* **1996**, *100*, 17820–17824.
[11] Belof, J. L. Theory and simulation of metal-organic materials and biomolecules. Ph.D. thesis, University of South Florida, 2009.
[12] Dinh, T.-L.; Huber, G. A. *Journal of Mathematical Modelling and Algorithms* **2005**, *4*, 111–128.
[13] Palmo, K.; Krimm, S. *Chemical Physics Letters* **2004**, *395*, 133–137.
[14] Metropolis, N.; Rosenbluth, A. W.; Rosenbluth, M. N.; Teller, A. H.; Teller, E. *Phys. Lett. B* **1953**, *21*, 1087–1092.
[15] McQuarrie, D. A. *Statistical Mechanics*; University Science Books: Sausalito, CA, 2000; Chapt. 3, pg. 53.
[16] Frenkel, D.; Smit, B. *Understanding Molecular Simulation: From Algorithms to Applications*; Academic Press: New York, 2002; Chapt. 5, Sect. 6.1, p.129.
[17] Boublík, T. *Fluid Phase Equil.* **2005**, *240*, 96–100.
[18] Jones, J. *Proceedings of the Royal Society of London. Series A, Containing Papers of a Mathematical and Physical Character* **1924**, *106*, 463–477.
[19] Ewald, P. P. *Annalen der Physik* **1921**, *369*, 253–287.
[20] Feynman, R. P.; Hibbs, A. R. *Quantum Mechanics and Path Integrals*; McGraw-Hill: New York, 1965; Chapt. 10, Sect. 3, pg. 281.
[21] Nicholson, D.; Parsonage, N. G. *Computer Simulation and the Statistical Mechanics of Adsorption*; Academic Press: London, 1982.
[22] Belof, J. L.; Space, B. Massively Parallel Monte Carlo (MPMC). Available on Google Code, 2012.
[23] Cornell, W. D.; Cieplak, P.; Bayly, C. I.; Gould, I. R.; Merz, K. M.; Ferguson, D. M.; Spellmeyer, D. C.; Fox, T.; Caldwell, J. W.; Kollman, P. A. *Journal of the American Chemical Society* **1995**, *117*, 5179–5197.
[24] Stevens, W. J.; Basch, H.; Krauss, M. *J. Chem. Phys.* **1984**, *81*, 6026.
[25] Hay, P. J.; Wadt, W. R. *J. Chem. Phys.* **1985**, *82*, 270.
[26] LaJohn, L. A.; Christiansen, P. A.; Ross, R. B.; Atashroo, T.; Ermler, W. C. *J. Chem. Phys.* **1987**, *87*, 2812.
[27] Singh, U. C.; Kollman, P. A. *Journal of Computational Chemistry* **1984**, *5*, 129–145.
[28] Belof, J. L.; Stern, A. C.; Space, B. *Journal of Chemical Theory and Computation* **2008**, *4*, 1332–1337.
[29] Buch, V. *The Journal of Chemical Physics* **1994**, *100*, 7610.
[30] Darkrim, F.; Levesque, D. *The Journal of Chemical Physics* **1998**, *109*, 4981.